Metabotropic NMDA receptor function is required for NMDA receptor-dependent long-term depression

Sadegh Nabavi[a,1], Helmut W. Kessels[a,b,1], Stephanie Alfonso[a], Jonathan Aow[a], Rocky Fox[a], and Roberto Malinow[a,2]

[a]Center for Neural Circuits and Behavior, Division of Biology, Department of Neuroscience and Section of Neurobiology, University of California at San Diego, La Jolla, CA 92093; and [b]Netherlands Institute for Neuroscience, Royal Netherlands Academy of Arts and Sciences, 1105 BA, Amsterdam, The Netherlands

Contributed by Roberto Malinow, November 8, 2012 (sent for review September 27, 2012)

NMDA receptor (NMDAR) activation controls long-term potentiation (LTP) as well as long-term depression (LTD) of synaptic transmission, cellular models of learning and memory. A long-standing view proposes that a high level of Ca^{2+} entry through NMDARs triggers LTP; lower Ca^{2+} entry triggers LTD. Here we show that ligand binding to NMDARs is sufficient to induce LTD; neither ion flow through NMDARs nor Ca^{2+} rise is required. However, basal levels of Ca^{2+} are permissively required. Lowering, but not maintaining, basal Ca^{2+} levels with Ca^{2+} chelators blocks LTD and drives strong synaptic potentiation, indicating that basal Ca^{2+} levels control NMDAR-dependent LTD and basal synaptic transmission. Our findings indicate that metabotropic actions of NMDARs can weaken active synapses without raising postsynaptic calcium, thereby revising and expanding the mechanisms controlling synaptic plasticity.

GluN2 | NR2 | BAPTA | AMPA receptor | ion-flux independent

Glutamate, the major excitatory transmitter in the brain, acts on several receptors that have been divided into ionotropic [(AMPA, NMDA, kainate) those whose primary function is to allow entry of ions into neurons] and metabotropic [(mGluR1-8) those that through conformational changes drive intracellular signaling pathways independent of ion-channel flow] classes (1, 2). Identification of selective NMDA receptor (NMDAR) antagonists (3) permitted ascribing its requirement (4) for the long-term potentiation (LTP) of synaptic transmission triggered by a high-frequency stimulus (5). Early studies also found that NMDARs were permeable to Ca^{2+} (6) and that LTP induction produces a rise in intracellular Ca^{2+} in postsynaptic sites (7). Furthermore, introduction of a Ca^{2+} chelator into the postsynaptic neuron blocked LTP (8). These studies provided a simple model that the NMDAR was selectively activated during a high-frequency stimulus and allowed entry of Ca^{2+} ions that initiated intracellular signaling, leading to LTP. A major question arose after the finding that a low-frequency stimulus (LFS) produced long-term depression (LTD) of synaptic transmission that was also blocked by an antagonist to NMDARs (9, 10). LTD was blocked by intracellular introduction of a calcium chelator, and rises in calcium were observed during LTD induction (11–13). Thus, a model was proposed in which a small rise in cytoplasmic calcium produced LTD, whereas high rises in calcium produced LTP (14–16). In addition to physiological processes, NMDAR-dependent LTD may participate in pathological conditions, in particular the synaptic depression produced by exposure of neurons to β-amyloid (Aβ). We sought to examine the role of NMDAR function in these forms of NMDAR-dependent synaptic depression [see the companion article in this issue (17)].

Results

NMDAR-Dependent LTD Is Independent of Ion Influx. NMDAR-dependent LTD was studied in acute hippocampal slices with field potential recordings of AMPA receptor (AMPAR)-mediated responses. Two independent pathways were monitored; robust depression was observed in the pathway receiving LFS, compared with a control pathway that received no LFS (Fig. 1*A*). As expected (9, 10), this form of LTD was blocked by 100 μM D-(-)-2-Amino-5-phosphonopentanoic acid (D-APV) (Fig. 1*B*), an NMDAR antagonist that blocks glutamate binding to the GluN2 subunit. To test whether ion flux through the NMDAR channel is required, we used the NMDAR ion-channel blocker MK-801. Slices were incubated for 3–4 h in 100 μM MK-801 and subsequently placed in a recording chamber containing 100 μM MK-801. After monitoring baseline transmission, an LFS was delivered to one pathway, which produced synaptic depression that was indistinguishable from that seen in the no-drug control conditions [Fig. 1*C*; cf. 18; but see Raymond et al. (19)]. Because NMDAR blockade by MK-801 is use-dependent, we conducted control experiments to rule out the possibility that the NMDAR channel was not fully blocked during the LTD induction protocol. These control experiments indicate that NMDAR-mediated synaptic currents are more than 99% blocked before an LTD protocol was delivered (Fig. 2*A*). Synaptic NMDARs are likely blocked in this experiment owing to the opening of NMDARs during the 3- to 4-h incubation period and the evoked transmission during the baseline period. These results indicate that LTD does not require ionic flux through synaptic NMDARs.

We examined further the requirements for LTD using 100 μM 7-chlorokynurenate (7CK), an antagonist at the glycine-binding site on the GluN1 subunit of NMDARs (20). 7CK fully blocked both synaptic and extrasynaptic NMDAR-mediated currents (Fig. S1). Even during an LTD induction protocol, which conceivably could release glycine and overcome the competitive block by 7CK, this drug prevents NMDAR channel opening (Fig. 2*B*). In the presence of 7CK LTD was still observed (Fig. 1*D*), supporting the view that ion flux through the NMDAR channel is not required for LTD. To rule out the possibility that in the presence of MK-801 or 7CK a different form of LTD was triggered [e.g., LTD requiring mGluR5 (21, 22) or voltage-gated calcium channels (11)], we included inhibitors of mGluR5 (3-[(2-Methyl-4-thiazolyl)ethynyl]pyridine [MTEP], 4 μM) and voltage-gated calcium channels (nifedipine, 100 μM) in the bath. Experiments with 7CK + MTEP + nifedipine showed LTD that was no different from those experiments using MK-801 or 7CK alone (Fig. 2*C*). The LTD remaining in the presence of 7CK was dependent on NMDARs: experiments in which we added both 7CK and D-APV displayed no LTD (Fig. 2*D*). Our results suggest that ligand binding to the NMDAR glutamate-binding site at the GluN2 subunit (which is blocked by D-APV) but not ion channel flow (which is blocked by MK-801 and 7CK) is necessary to induce LTD.

LTD generally requires long induction protocols (e.g., LFS for 15 min). If ligand binding to NMDARs is sufficient to

Author contributions: S.N., H.W.K., and R.M. designed research; S.N., H.W.K., S.A., J.A., and R.F. performed research; S.N. and H.W.K. analyzed data; and S.N., H.W.K., and R.M. wrote the paper.

The authors declare no conflict of interest.

[1]H.W.K. and S.N. contributed equally to this work.

[2]To whom correspondence should be addressed. E-mail: rmalinow@ucsd.edu.

This article contains supporting information online at www.pnas.org/lookup/suppl/doi:10.1073/pnas.1219454110/-/DCSupplemental.

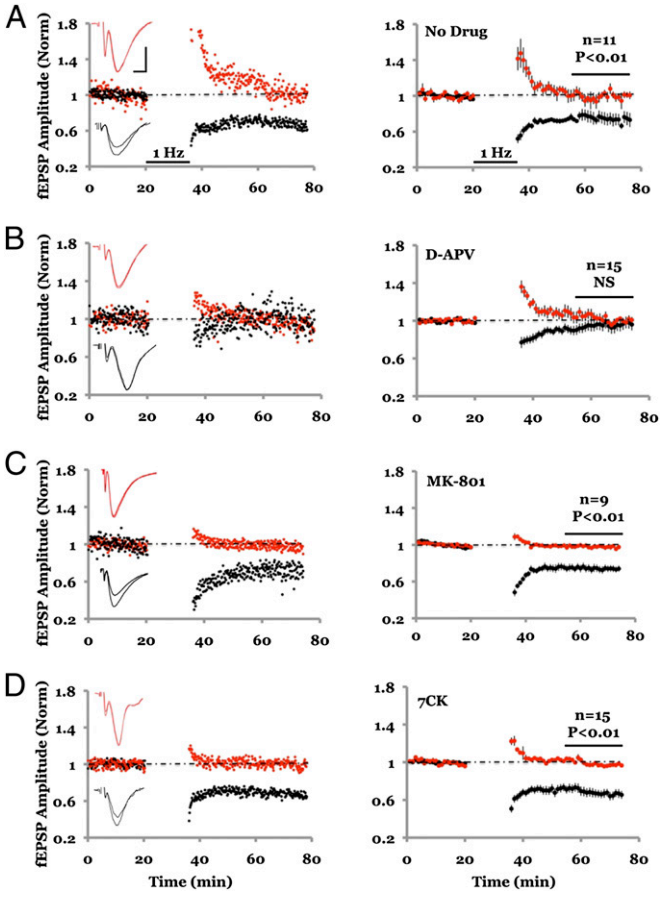

Fig. 1. NMDAR-dependent LTD requires ligand binding but not ion-channel flux through NMDAR. (*A*) Field potential recordings from two independent pathways; one pathway (black symbols) received a 1-Hz, 15-min stimulus where indicated. The control pathway (red symbols) received no stimulus. (*Left*) Individual experiment; (*Right*), collated average. (*Inset*) Average field responses obtained before and after LFS delivery. (*B*) LFS-induced depression is blocked by inclusion of 100 μM D-APV in the bath. (*C*) LFS-induced depression is not blocked by 100 μM MK-801. Slices were incubated for 3–4 h in 100 μM MK-801 before transfer to the recording chamber, which also included 100 μM MK-801. (*D*) LFS-induced depression is not blocked by inclusion of 100 μM 7CK in the bath. In approximately half of the experiments shown in *A*, *B*, *C*, and *D* 4 μM MTEP was included in the bath to rule out the possible involvement of mGluR5; there was no difference in results with and without MTEP (Fig. S5). Error bars throughout represent SEM. Statistics throughout: paired *t* test when comparing cell pairs; unpaired *t* test when comparing across different slices. (Scale bars, 0.3 mV, 5 ms.)

induce LTD, we reasoned that brief, high-frequency stimuli could induce LTD as long as calcium entry through NMDARs (and LTP) was blocked. We tested this prediction by delivering 100-Hz tetanic conditioning stimuli in the presence of MK-801 (Fig. 3). Indeed, whereas 100 Hz tetani in the absence of MK-801 produced LTP, in the presence of MK-801 100 Hz tetani produced LTD.

To examine signaling triggered by ligand binding to NMDARs we measured p38 MAPK activation in dissociated cultured neurons. Previous studies have implicated p38 MAPK signaling in LTD (23). Cultured neurons transiently exposed to NMDA produced an increase in p38 MAPK phosphorylation (Fig. 4). This increase in p38 MAPK phosphorylation was blocked by D-APV but not by MK-801. These results indicate that NMDARs can drive ligand-dependent, ion-channel independent signaling (i.e., metabotropic signaling).

Impact of Calcium Chelators on Synaptic Transmission. Our results indicating that ion flux through the NMDAR channel is not required for NMDAR-dependent LTD are consistent with predictions based on calcium dynamics in spines during LFS (24) but run counter to conclusions reached by previous studies in

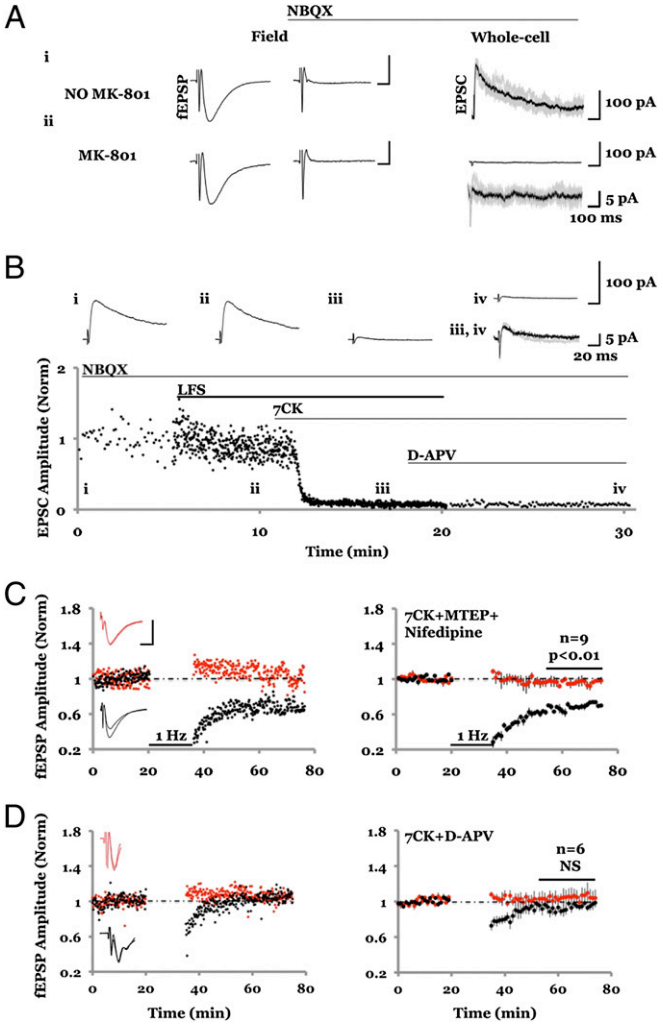

Fig. 2. MK-801 and 7CK fully block NMDAR-mediated responses even during LTD induction. (*A*, *Left*) Average of five AMPAR-mediated field responses in the absence of MK-801; 10 μM NBQX was added (*A*, *Center*), and whole-cell responses were obtained at holding potential of +40 mV displaying (*A*, *Right*) the first five evoked NMDAR-mediated responses (gray lines) along with an average (black line). (Scale bars, *Left*, 0.3 mV, 5 ms; *Right*, 100 pA, 100 ms.) The integrated NMDA current relative to the integrated (AMPAR-mediated) field potential was 6.5×10^3 pA/mV. (*A*, *ii*) Same as *A, i* but slices were incubated in 100 μM MK-801 for 2 h before and during recordings, producing an integrated NMDA current to integrated AMPAR-mediated field potential of 16.5 pA/mV. (*B*) Plot of NMDAR-mediated whole-cell response vs. time. (*Inset*) Average of 10 responses obtained where indicated. Note little difference between *B, iii* and *B, iv*, indicating that 7CK completely blocks NMDAR-mediated response, even during LFS. For *A* and *B* similar results were obtained in two independent experiments. (*C* and *D*) Field potential recordings with one pathway (black symbols) receiving a 1-Hz, 15-min stimulus where indicated, and the other control pathway (red symbols) receiving no stimulus. (*Left*) Individual experiment; (*Right*) collated average. (*Inset*) Average field responses obtained before and after LFS delivery. (Scale bars, 0.3 mV, 5 ms.) (*C*) LFS-induced depression is not blocked by inclusion of 7CK (100 μM) + MTEP (4 μM) + nifedipine (100 μM). (*D*) LFS-induced depression is blocked by inclusion of 7CK (100 μM) + D-APV (100 μM).

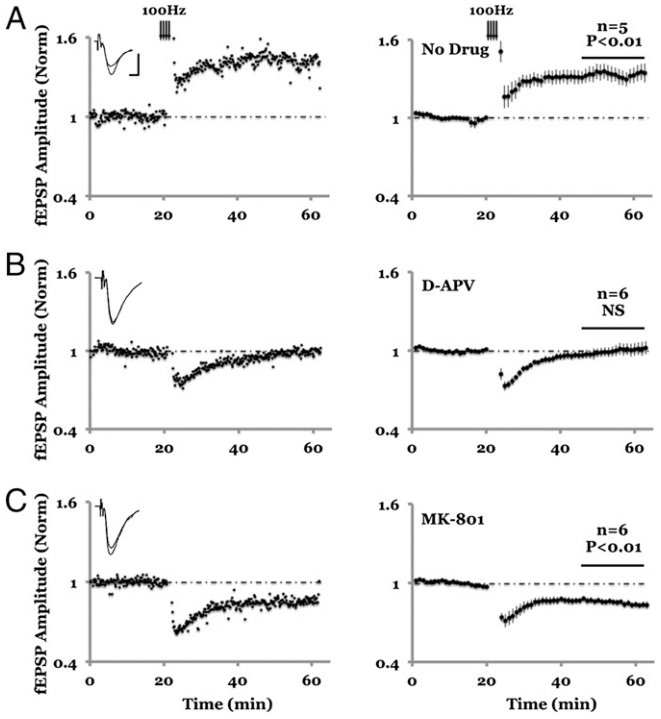

Fig. 3. Blockade of ion flux through NMDAR reverses the direction of synaptic plasticity induced by 100 Hz stimulation. (*A*) In the absence of NMDAR antagonist, 100 Hz tetani (arrows) induced LTP of the field potential, which is fully blocked by 100 μm D-APV (*B*). Inclusion of 100 μM MK-801, however, causes a long lasting depression (*C*). (*Left*) Individual experiment; (*Right*) Collated average. (*Inset*) Average field responses obtained before and after tetani delivery. (Scale bars, 0.3 mV, 5 ms.)

which calcium chelators were used to block LTD (11–13). We thus examined the impact of intracellular infusion of calcium chelators on synaptic transmission. We obtained simultaneous whole-cell recordings from two nearby cells: one cell with a standard internal solution (which contains 0.6 mM EGTA) that does not block LTD (13), whereas for the other cell the internal solution was supplemented with a high concentration (15 mM) of calcium chelator 1,2-bis(o-aminophenoxy)ethane-N,N,N′,N′-tetraacetic acid (BAPTA), which is known to block LTD (11). AMPAR-mediated synaptic transmission in the cell containing 15 mM BAPTA was markedly potentiated (Fig. 5*A*), within minutes of whole-cell access (Fig. S2). Transmission onto the cell with the standard 0.6-mM EGTA internal solution remained constant throughout. This effect of 15 mM BAPTA was similar to that of 15 mM EGTA (Fig. 5*C*) and was selective for AMPAR-mediated transmission because NMDAR-mediated transmission, monitored at +40 mV, was not affected (Fig. 5*B*).

How does 15 mM BAPTA enhance transmission? Addition of 15 mM BAPTA to the cytosol of a neuron reduced basal levels of intracellular calcium (Fig. S3 *A* and *B*). To test whether this was the cause for enhanced transmission, we added 1.3 mM Ca^{2+} to the internal solution containing 15 mM BAPTA, to maintain cellular free Ca^{2+} at a level comparable to that seen with 0.6 mM EGTA (Fig. S3 *A* and *B*), which is close to basal levels previously observed in hippocampal pyramidal neurons (25). In contrast to the effects of 15 mM BAPTA alone, infusion of 15 mM BAPTA with 1.3 mM Ca^{2+} produced no significant potentiation of AMPAR-mediated transmission compared with transmission onto a cell containing 0.6 mM EGTA (Fig. 5*D*). These results suggest that basal calcium maintains a constitutively active process that acts to reduce AMPAR-mediated synaptic transmission; upon lowering cytoplasmic calcium this process is blocked, effectively enhancing AMPAR-mediated transmission. One possibility is that basal calcium acts to restrict access of AMPARs to the synapse, as has been seen for recombinant GluA1-containing receptors (26, 27). Indeed, infusion of 15 mM BAPTA produced no synaptic potentiation in tissue from mice lacking GluA1 (Fig. 5 *G* and *H*), supporting the view that basal calcium acts to restrict GluA1-containing AMPARs from synapses.

How do basal levels of Ca^{2+} maintain reduced synaptic transmission? We hypothesized an action through active calcineurin, which is thought to produce depression of AMPAR-mediated transmission (28). To test this possibility we infused the calcineurin inhibitor FK506 into one of two simultaneously recorded neurons. After whole-cell access, the neuron containing FK506 showed synaptic potentiation (Fig. 5*E*; cf. 29). Furthermore, incubating slices with FK506 for 1–2 h significantly reduced the potentiation produced by intracellular infusion of 15 mM BAPTA (Fig. 5*F*), suggesting that these two manipulations use similar mechanisms. These results suggest that lowering basal levels of free Ca^{2+} reduces basal levels of calcineurin activity, thereby inhibiting a process that normally acts to reduce AMPAR-mediated transmission.

NMDAR-Dependent LTD Does Not Require a Ca^{2+} Rise. We hypothesized that the process keeping AMPAR-mediated synaptic transmission at a reduced level is required for NMDAR-dependent LTD to be generated. In this model, infusion of 15 mM BAPTA blocks this depressive process and thereby prevents LTD. To test this model we examined LTD in conditions whereby intracellular calcium could be controlled with whole-cell recordings. NMDAR-dependent LTD was obtained (22) with 0.6 mM EGTA and blocked with 15 mM BAPTA or 15 mM EGTA in the internal solution, as previously reported (11) (Fig. 6 *A* and *B* and Fig. S4). To test our model we used 15 mM BAPTA and 1.3 mM Ca^{2+} in the internal solution, which maintains intracellular free Ca^{2+} levels close to physiological levels (Fig. S3 *A* and *B*) and maintains a buffering capacity similar to 15 mM BAPTA with no added Ca^{2+} (Fig. S3*C*). In these conditions LTD was obtained, comparable in magnitude to that seen when using 0.6 mM EGTA in the internal solution (Fig. 6*C*). As an additional test to our model, we induced LFS conditioning while

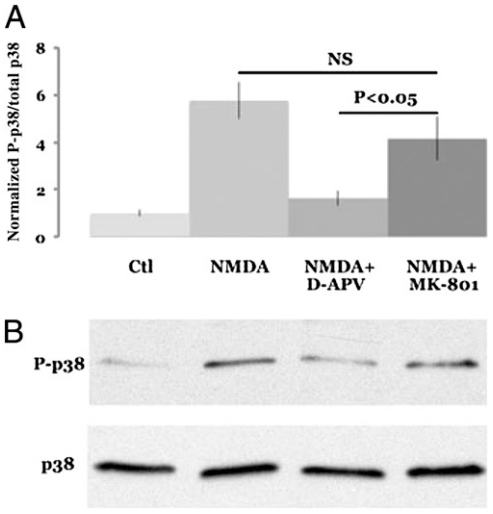

Fig. 4. NMDAR-dependent phosphorylation of p38 requires ligand binding but not ion-channel flux through NMDAR. (*A*) NMDA (40 μM) increase p38 phosphorylation (NMDA), which is largely blocked by 100 μM D-APV (NMDA+ D-APV) but not by 100 μM MK-801 (NMDA+MK-801). Magnitude of p38 phosphorylation is normalized to the no-treatment (Ctl). (*B*) Individual experiment (n = 12).

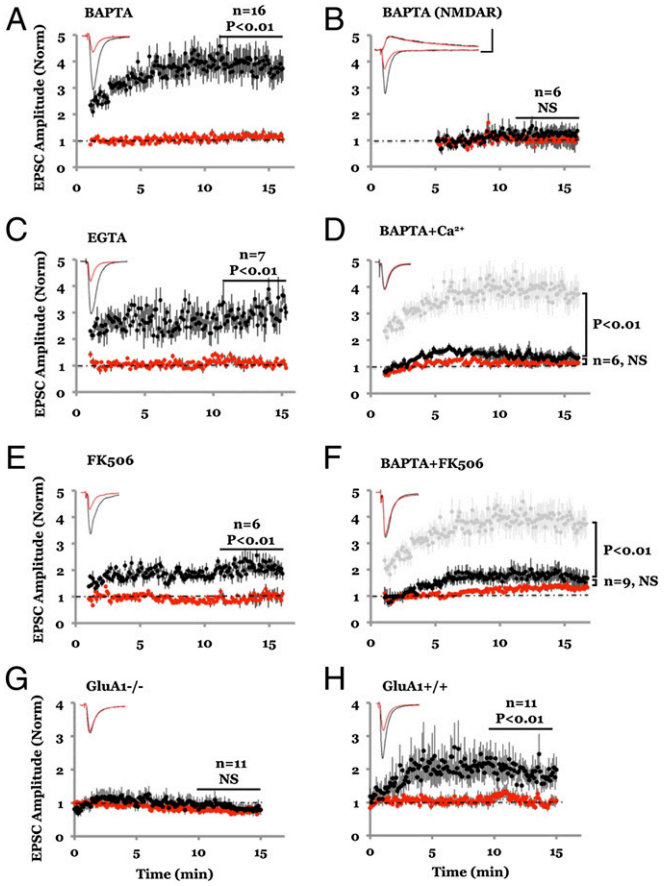

Fig. 5. Lowering cytoplasmic Ca^{2+} level with high chelator concentration selectively enhances AMPAR-mediated synaptic transmission. (*A*) Amplitude plot of AMPAR-mediated transmission from two nearby CA1 hippocampal pyramidal neurons obtained by simultaneous whole-cell recordings (holding potential at −60 mV) with internal solution containing 0.6 mM EGTA (red symbols) or 15 mM BAPTA (black symbols). (*Inset*) Average responses simultaneously recorded from the two cells. (*B*) Same as *A* for NMDAR-mediated transmission (holding potential at +40 mV). Note the large discrepancy in AMPAR-mediated responses with similar NMDAR-mediated responses from the two neurons. (*C*) Same as *A* but cells contain 0.6 mM EGTA (red) and 15 mM EGTA (black). (*D*) Same as *A* but cells contain 0.6 mM EGTA (red) and 15 mM BAPTA + 1.3 mM Ca^{2+} (black); light gray symbols show synaptic responses to 15 mM BAPTA (from *A*) for comparison. (Scale bars, 200 pA, 20 ms.) (*E*) Same as *A* but one cell (black) contained 100 μM FK-506 in the internal solution (0.6 mM EGTA in both cells). (*F*) Same as *A* but slices were incubated prior (1–2 h) and during whole-cell recordings with 100 μM FK-506 in the bath. Light gray symbols indicate responses (from *A*) in the absence of FK-506 for comparison. (*G*) BAPTA failed to induce synaptic potentiation (black) in mice lacking GluA1 ($GluA1^{-/-}$); however, it was effective in the wild-type littermates ($GluA1^{+/+}$).

holding the membrane potential at −80 mV to minimize NMDAR currents (30). In this case we also obtained LTD, suggesting that relief of the voltage-dependent Mg^{2+} block of NMDA receptors to allow ion flux is not required for LTD (Fig. 6*D*). These results indicate that LTD requires intracellular free Ca^{2+} to be at basal levels but does not need free Ca^{2+} to rise above basal levels. We conclude that NMDAR-dependent LTD can be induced with no rise in postsynaptic free Ca^{2+}.

Discussion

In this study we have examined the role of the NMDAR in NMDAR-dependent LTD. We find that whereas an antagonist at the glutamate-binding site of the NMDAR blocks this form of depression, antagonists at the glycine-binding site (7CK) or at the channel pore (MK-801) do not. This failure to block synaptic depression is not due to a lack of NMDAR block by MK-801 or 7CK or to the recruitment of other forms of non-NMDAR–dependent synaptic depression. Our findings indicate that ion flux through the NMDAR is not required for NMDAR-dependent depression of synaptic AMPARs to occur. We propose that glutamate binding to the NMDAR during an LFS produces conformational changes in its GluN2 subunits, which are linked to intracellular signaling pathways (independent of ion flux) that generate LTD. Such Ca^{2+} flux-independent (i.e., metabotropic) NMDAR signaling is also required for Aβ-driven synaptic depression [see the companion article in this issue (17)]. Our results suggest that activation of p38 MAPK is one signal produced by metabotropic activation of NMDARs.

Our conclusions run counter to the widely held view that low levels of Ca^{2+} passing through the NMDAR are necessary to trigger LTD—a view primarily based on the use of calcium chelators (11–13). Indeed, we confirm that infusion of a cell with 15 mM BAPTA does block LTD. However, infusion of a cell with 15 mM BAPTA reduces free cytoplasmic Ca^{2+} and produces a large potentiation of AMPAR-mediated transmission, effects not produced by 15 mM BAPTA + 1.3 mM Ca^{2+}. Thus,

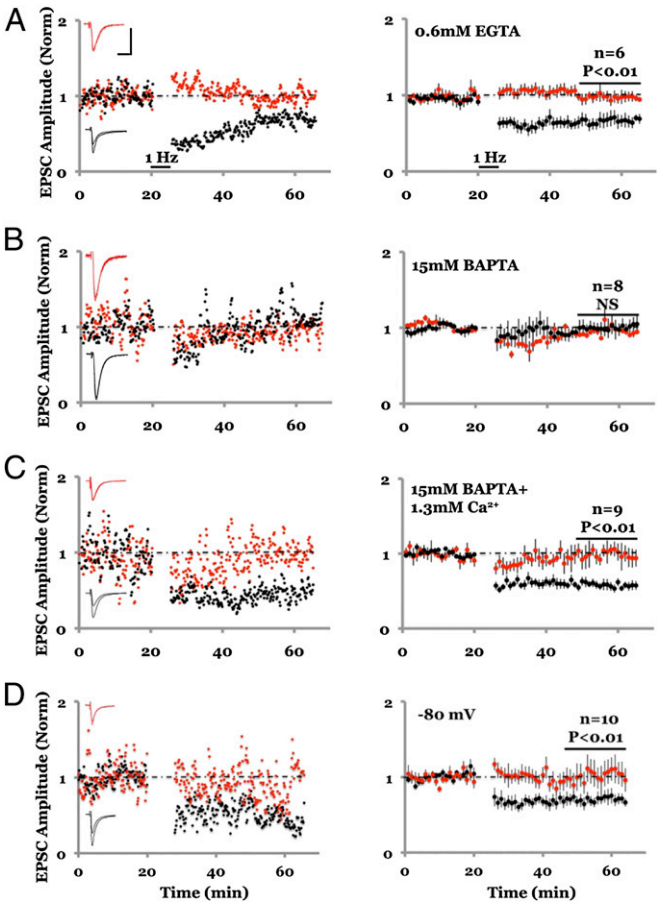

Fig. 6. Clamping intracellular Ca^{2+} to basal levels does not block LTD. (*A–D*) Plot of whole-cell synaptic responses with internal solution containing 0.6 mM EGTA; LFS delivered to one path (black symbols) where indicated; control path not stimulated (red symbols). (*Left*) Individual experiment; (*Right*) collated averages; error bars SEM. (*A*) LFS induces stable LTD. (*B*) LTD is blocked with internal solution containing 15 mM BAPTA. (*C*) LTD is not blocked with internal solution containing 15 mM BAPTA + 1.3 mM Ca^{2+}. (*D*) Hyperpolarization to −80 mV during LFS does not inhibit LTD.

lowering basal calcium seems to remove a check on basal transmission that normally maintains AMPAR-mediated transmission at a low level. This check is mediated by the actions of basal calcineurin activity because infusion of FK506 also produces synaptic potentiation that occludes the potentiation produced by 15 mM BAPTA. This check requires GluA1, which is known to participate in LTD (31). We conclude that calcium chelators are not simply clamping cytoplasmic Ca^{2+} levels; they are lowering Ca^{2+} levels and thereby modifying cellular processes that control synaptic transmission and plasticity. Indeed, when we use calcium chelators to clamp cytoplasmic Ca^{2+} to near-baseline levels, we see no block of LFS-induced LTD. Thus, previous studies using Ca^{2+} chelators do not argue against ion flux-independent LFS-induced LTD.

A previous study showed that hyperpolarization of the postsynaptic cell to −105 mV during a conditioning LFS can block LTD (10). The authors interpreted this to mean that a voltage-dependent Mg^{2+} block of ion flux through the NMDAR is required for LTD. An alternative explanation is that hyperpolarization to −105 mV can affect the conformation of the NMDAR such that it cannot undergo transitions that are required for LTD signaling to occur. The observed voltage dependence of NMDAR function that is independent of Mg^{2+} (32) is consistent with this latter view.

Our study supports the view that a rise in cytoplasmic calcium is not required for NMDAR-dependent LTD. This is not inconsistent with the view that there can be circumstances in which a cytoplasmic Ca^{2+} rise can produce synaptic depression. Indeed a rise in calcium produced by a series of depolarizing steps (11) or by photolysis of "caged calcium" (33) can produce synaptic depression that can occlude LTD. In agreement with this view, our study indicates that basal levels of calcium control synaptic transmission in such a way that lowering Ca^{+2} enhances transmission; a transient rise in calcium by various manipulations could well lower synaptic transmission.

Our findings suggest unique mechanisms underlying synaptic plasticity. We show that synaptic weakening can be induced by repetitive activation of NMDARs with no rise in postsynaptic Ca^{2+}. Indeed, high-frequency synaptic activation can produce LTD if the ion flux through the NMDAR is blocked. This may normally occur when a synapse is hyperactive while surrounding synapses onto the same cell are inactive; or when excitatory synapses are active during inhibitory tone. The link between conformational changes in the NMDAR and the signaling (34–36) causing depression of AMPAR-mediated responses remains to be elucidated. Basal calcium may be acting through hippocalcin, a calcium-sensitive protein that is required for LTD (37). Previous studies showed that ligand-binding of the NMDAR produces NMDAR endocytosis (38) and switch of GluN2B- to GluN2A-containing NMDARs (39): the role of such processes in LTD will need to be examined. It is notable that sizable synaptic strengthening can be produced by decreasing the levels of intracellular Ca^{2+}; this could constitute a molecular mechanism underlying homeostatic plasticity (40, 41) (i.e., prolonged silencing of neuronal activity could act to lower basal levels of Ca^{2+} and thereby enhance transmission). The phenomena we have identified add to the rich list of mechanisms that control normal synaptic plasticity and may participate in pathophysiological conditions, such as those produced by excessive Aβ [see the companion article in this issue (17)].

Experimental Procedures

Organotypic and Acute Hippocampal Slices. Organotypic hippocampal slices were prepared from 6- to 7-d-old rat pups as described previously (26) and used at 6–9 days in vitro (DIV). Acute hippocampal slices were prepared from 2- to 3-wk-old Sprague-Dawley rats. Slices were cut in cold sucrose cutting solution containing, in mM, sucrose 72, glucose 22, $NaHCO_3$ 2.6, NaCl 83, KCl 2.5, $MgSO_4$ 3.3, and $CaCl_2$ 0.5. Slices were transferred to a recovery chamber containing artificial cerebrospinal fluid (ACSF) solution supplemented with 11 mM glucose, 1 mM $MgCl_2$, and 2 mM $CaCl_2$ and maintained at 35 °C for 45 min and subsequently at room temperature for at least 45 min. The CA3 region was surgically removed in organotypic slices to prevent stimulus-induced bursting. A slice was transferred to the recording chamber, where it was submerged with continuous flow of ACSF, containing 119 mM NaCl, 2.5 mM KCl, 26 mM $NaHCO_3$, 1 mM NaH_2PO_4, 11 mM glucose, 100 μM picrotoxin (pH 7.4), supplemented with 1 mM $MgCl_2$, and 2 mM $CaCl_2$ (acute slice) or 4 mM $CaCl_2$, 4 mM $MgCl_2$, and 4 μM 2-chloroadenosine (organotypic slice). All experiments were performed at 24–28 °C.

Dissociated Cortical Cultures and Immunoblot for Phospho-p38. Primary neuronal culture was prepared from postnatal day 2 (P2) Sprague-Dawley rat pups with papain digestion and mechanical trituration (42). Cells were plated on poly-D-lysine–coated glass-bottom dishes (MatTek). At 14 DIV, neurons were treated with 40 μM NMDA solution for 3 min (43). Cell lysates were prepared with radioimmunoprecipitation assay buffer containing 50 mM Tris·HCl (pH 8), 150 mM NaCl, 1% Nonidet P-40, 0.5% sodium deoxycholate, 0.1% SDS, 2% (vol/vol) protease inhibitor (Roche), and 1% of phosphatase inhibitors mixtures II and III (Sigma). Lysates were cleared at 16,100 × *g* for 15 min. After measuring the concentration (BCA assay kit; Thermo Scientific), 20 μg of protein per lane was loaded on SDS/PAGE gels (4–20%; Bio-Rad). The resulting gel was transferred to the transfer membrane (Millipore). The membranes were incubated with anti-phospho-p38 MAPK (Cell Signaling) at 4 °C overnight. Phospho-p38 antibody was removed by incubating the membranes in the stripping solution [2% SDS, 62.5 mM Tris·HCl (pH 6.8), and 114 mM β mercaptoethanol] for 30 min at 50 °C and reprobed with anti-p38 MAPK. The relative amount of p38 phosphorylation (Thr180/Tyr182) was calculated by taking the ratio of phospho-p38 to p38.

Electrophysiology. Whole-cell recordings were obtained from individual or pair of neighboring cells in CA1 region using glass pipettes (3–6 MΩ) filled with internal solution containing, in mM, K-gluconate 170, Hepes 10, NaCl 5, KCl 10, EGTA 0.6, Na_2GTP 2, and NaGTP 0.3. Where K_4-BAPTA (15 mM) or K_2-EGTA (15 mM) was loaded into cells, equimolar amount of K-gluconate was replaced. For experiments shown in Figs. 2 *A* and *B*, 5*B*, and 6*D* and Fig. S1, K-Gluconate was substituted with equimolar Cs-methanesulfonate. Synaptic responses were evoked by stimulating two independent pathways using bipolar stimulating electrodes (Frederick Haer) placed 150–250 μm down the apical dendrites, 100 μm apart, and 150–200 μm laterally in opposite directions. For excitatory postsynaptic currents (EPSC) measurements from paired recordings, results from two pathways were averaged and analyzed as $n = 1$; cell pairs with more than 20% difference in series resistance were excluded. The AMPAR-mediated EPSC was measured by averaging a fixed 3-ms window covering the peak amplitude and subtracting from an average current window before stimulation. NMDAR-mediated response, measured as total charge, was calculated by integrating the area under response curve.

Extracellular field potential was recorded in stratum radiatum with glass electrodes (1–2 MΩ) filled with the perfusion solution. Field excitatory postsynaptic potential was measured by averaging the response over a 5-ms fixed window covering the peak amplitude. 2,3-dihydroxy-6-nitro-7-sulfamoyl-benzo[f]quinoxaline-2,3-dione (NBQX) (10 μM) was added at the end of most experiments, and responses were subtracted from the responses before drug addition.

Whole-cell voltage clamp LTD was induced as described by Terashima et al. (44). After a minimum of 30-min baseline EPSCs recorded at −60 mV by stimulating afferents at 0.1 Hz, LTD was induced in one of two independent pathways by applying 300 stimuli at 1 Hz at holding potential of −40 mV, except for Fig. 6*D*, in which holding potential was set at −80 mV. Recording was terminated if input resistance decreased or series resistance increased by more than 20%. Experiments were excluded if control pathway, at 30 min after induction to the test pathway, decreased by more than 10% of its baseline.

Extracellular field LTD was induced as described previously (9, 10). After 20-min baseline (or 40 min when MK-801 was used), established by stimulating two independent pathways at 0.1 Hz, LTD was induced in one pathway by applying 900 pulses at 1 Hz. Experiments were excluded if control pathway, 30 min after induction to the test pathway, decreased by more than 10% of its baseline or there was a 10% change between the first and last 5 min of the 20-min baseline of test pathway.

Extracellular field LTP was induced as described previously (11) after 20-min baseline (or 40 min when MK-801 was used), established by stimulating at 0.1 Hz. The amplitude of the field potential was adjusted to 0.4–0.8 mV corresponding to a stimulus strength of less than 50% of the maximal field response. LTP was induced by applying 4 trains, 20 s apart, of 100 Hz tetanus with 1-s duration.

Calcium Imaging. Free calcium concentration and calcium buffering capability were measured in pyramidal neurons in CA1 region from acute slices of 2- to 3-wk-old rats. For Fig. S3*A*, we performed dual indicator-based (25, 45) two-photon laser scanning microscopic imaging (Prairie Tech., Coherent Tech.), using Ca^{2+} sensitive Oregon green BAPTA (G, 100 μM) and Ca^{2+} insensitive Alexa-594 (R, 20 μM). We calibrated the system by measuring G/R max and G/R min (including 2 mM Ca or 2 mM BAPTA, respectively) in a recording pipet. We then measured G and R in neurons perfused with different Ca^{2+} buffers (as in Fig. S3) and used the equation

$$\left[Ca^{2+}\right]/K_D = \left\{(G/R) - (G/R)_{\min}\right\}/\left\{(G/R)_{\max} - (G/R)\right\}$$

to determine the free cytoplasmic Ca^{2+} levels. The K_D value for Ca^{2+} binding to Oregon Green BAPTA is 290 nM (45). Images were taken 10–20 min after whole-cell access was obtained. To measure the ability of neurons to buffer a calcium transient, neurons were loaded with different internal solutions (as per Fig. S3) along with 100 μM FURA-2. Images were captured at ∼0.1 Hz (Till Photonics) before, during, and after a 1-s train of 50 action potentials. Cell body fluorescence was background subtracted, and deltaF/F was calculated relative to the first image.

Sources of Drugs. NMDAR and AMPAR antagonists were from Tocris Bioscience; BAPTA, Oregon Green BAPTA, and FURA-2 were from Invitrogen; EGTA was from Amresco. All other drugs were from Sigma.

ACKNOWLEDGMENTS. We thank I. Hunton for technical assistance and J. Isaacson for comments on the manuscript and contributing to the data shown in Fig. S3. This work was supported by the National Institutes of Health and the Shiley-Marcos Foundation.

1. Traynelis SF, et al. (2010) Glutamate receptor ion channels: Structure, regulation, and function. *Pharmacol Rev* 62(3):405–496.
2. Niswender CM, Conn PJ (2010) Metabotropic glutamate receptors: Physiology, pharmacology, and disease. *Annu Rev Pharmacol Toxicol* 50:295–322.
3. Davies J, Francis AA, Jones AW, Watkins JC (1981) 2-Amino-5-phosphonovalerate (2APV), a potent and selective antagonist of amino acid-induced and synaptic excitation. *Neurosci Lett* 21(1):77–81.
4. Collingridge GL, Kehl SJ, McLennan H (1983) Excitatory amino acids in synaptic transmission in the Schaffer collateral-commissural pathway of the rat hippocampus. *J Physiol* 334:33–46.
5. Bliss TV, Lomo T (1973) Long-lasting potentiation of synaptic transmission in the dentate area of the anaesthetized rabbit following stimulation of the perforant path. *J Physiol* 232(2):331–356.
6. MacDermott AB, Mayer ML, Westbrook GL, Smith SJ, Barker JL (1986) NMDA-receptor activation increases cytoplasmic calcium concentration in cultured spinal cord neurones. *Nature* 321(6069):519–522.
7. Regehr WG, Tank DW (1990) Postsynaptic NMDA receptor-mediated calcium accumulation in hippocampal CA1 pyramidal cell dendrites. *Nature* 345(6278):807–810.
8. Lynch G, Larson J, Kelso S, Barrionuevo G, Schottler F (1983) Intracellular injections of EGTA block induction of hippocampal long-term potentiation. *Nature* 305(5936): 719–721.
9. Dudek SM, Bear MF (1992) Homosynaptic long-term depression in area CA1 of hippocampus and effects of N-methyl-D-aspartate receptor blockade. *Proc Natl Acad Sci USA* 89(10):4363–4367.
10. Mulkey RM, Malenka RC (1992) Mechanisms underlying induction of homosynaptic long-term depression in area CA1 of the hippocampus. *Neuron* 9(5):967–975.
11. Cummings JA, Mulkey RM, Nicoll RA, Malenka RC (1996) Ca2+ signaling requirements for long-term depression in the hippocampus. *Neuron* 16(4):825–833.
12. Bröcher S, Artola A, Singer W (1992) Intracellular injection of Ca2+ chelators blocks induction of long-term depression in rat visual cortex. *Proc Natl Acad Sci USA* 89(1): 123–127.
13. Cho K, Aggleton JP, Brown MW, Bashir ZI (2001) An experimental test of the role of postsynaptic calcium levels in determining synaptic strength using perirhinal cortex of rat. *J Physiol* 532(Pt 2):459–466.
14. Lisman J (1989) A mechanism for the Hebb and the anti-Hebb processes underlying learning and memory. *Proc Natl Acad Sci USA* 86(23):9574–9578.
15. Malenka RC, Nicoll RA (1993) NMDA-receptor-dependent synaptic plasticity: Multiple forms and mechanisms. *Trends Neurosci* 16(12):521–527.
16. Artola A, Singer W (1993) Long-term depression of excitatory synaptic transmission and its relationship to long-term potentiation. *Trends Neurosci* 16(11):480–487.
17. Kessels HW, Nabavi S, Malinow R (2013) Metabotropic NMDA receptor function is required for β-amyloid–induced synaptic depression. *Proc Natl Acad Sci* 110: 4029–4034.
18. Mayford M, Wang J, Kandel ER, O'Dell TJ (1995) CaMKII regulates the frequency-response function of hippocampal synapses for the production of both LTD and LTP. *Cell* 81(6):891–904.
19. Raymond CR, Ireland DR, Abraham WC (2003) NMDA receptor regulation by amyloid-beta does not account for its inhibition of LTP in rat hippocampus. *Brain Res* 968(2): 263–272.
20. Kemp JA, et al. (1988) 7-Chlorokynurenic acid is a selective antagonist at the glycine modulatory site of the N-methyl-D-aspartate receptor complex. *Proc Natl Acad Sci USA* 85(17):6547–6550.
21. Stanton PK, Chattarji S, Sejnowski TJ (1991) 2-Amino-3-phosphonopropionic acid, an inhibitor of glutamate-stimulated phosphoinositide turnover, blocks induction of homosynaptic long-term depression, but not potentiation, in rat hippocampus. *Neurosci Lett* 127(1):61–66.
22. Oliet SH, Malenka RC, Nicoll RA (1997) Two distinct forms of long-term depression coexist in CA1 hippocampal pyramidal cells. *Neuron* 18(6):969–982.
23. Zhu JJ, Qin Y, Zhao M, Van Aelst L, Malinow R (2002) Ras and Rap control AMPA receptor trafficking during synaptic plasticity. *Cell* 110(4):443–455.
24. Sabatini BL, Oertner TG, Svoboda K (2002) The life cycle of Ca(2+) ions in dendritic spines. *Neuron* 33(3):439–452.
25. Maravall M, Mainen ZF, Sabatini BL, Svoboda K (2000) Estimating intracellular calcium concentrations and buffering without wavelength ratioing. *Biophys J* 78(5): 2655–2667.
26. Shi SH, et al. (1999) Rapid spine delivery and redistribution of AMPA receptors after synaptic NMDA receptor activation. *Science* 284(5421):1811–1816.
27. Makino H, Malinow R (2009) AMPA receptor incorporation into synapses during LTP: The role of lateral movement and exocytosis. *Neuron* 64(3):381–390.
28. Mulkey RM, Endo S, Shenolikar S, Malenka RC (1994) Involvement of a calcineurin/inhibitor-1 phosphatase cascade in hippocampal long-term depression. *Nature* 369(6480):486–488.
29. Wang JH, Kelly PT (1997) Postsynaptic calcineurin activity downregulates synaptic transmission by weakening intracellular Ca2+ signaling mechanisms in hippocampal CA1 neurons. *J Neurosci* 17(12):4600–4611.
30. Gray JA, et al. (2011) Distinct modes of AMPA receptor suppression at developing synapses by GluN2A and GluN2B: Single-cell NMDA receptor subunit deletion in vivo. *Neuron* 71(6):1085–1101.
31. Lee HK, Takamiya K, He K, Song L, Huganir RL (2010) Specific roles of AMPA receptor subunit GluR1 (GluA1) phosphorylation sites in regulating synaptic plasticity in the CA1 region of hippocampus. *J Neurophysiol* 103(1):479–489.
32. Clarke RJ, Johnson JW (2008) Voltage-dependent gating of NR1/2B NMDA receptors. *J Physiol* 586(Pt 23):5727–5741.
33. Yang SN, Tang YG, Zucker RS (1999) Selective induction of LTP and LTD by postsynaptic [Ca2+]i elevation. *J Neurophysiol* 81(2):781–787.
34. Malinow R, Malenka RC (2002) AMPA receptor trafficking and synaptic plasticity. *Annu Rev Neurosci* 25:103–126.
35. Sheng M, Kim MJ (2002) Postsynaptic signaling and plasticity mechanisms. *Science* 298 (5594):776–780.
36. Collingridge GL, Peineau S, Howland JG, Wang YT (2010) Long-term depression in the CNS. *Nat Rev Neurosci* 11(7):459–473.
37. Palmer CL, et al. (2005) Hippocalcin functions as a calcium sensor in hippocampal LTD. *Neuron* 47(4):487–494.
38. Vissel B, Krupp JJ, Heinemann SF, Westbrook GL (2001) A use-dependent tyrosine dephosphorylation of NMDA receptors is independent of ion flux. *Nat Neurosci* 4(6): 587–596.
39. Barria A, Malinow R (2002) Subunit-specific NMDA receptor trafficking to synapses. *Neuron* 35(2):345–353.
40. Davis GW, Bezprozvanny I (2001) Maintaining the stability of neural function: A homeostatic hypothesis. *Annu Rev Physiol* 63:847–869.
41. Turrigiano GG, Leslie KR, Desai NS, Rutherford LC, Nelson SB (1998) Activity-dependent scaling of quantal amplitude in neocortical neurons. *Nature* 391(6670): 892–896.
42. Bekkers JM (2005) Presynaptically silent GABA synapses in hippocampus. *J Neurosci* 25(16):4031–4039.
43. Lee HK, Kameyama K, Huganir RL, Bear MF (1998) NMDA induces long-term synaptic depression and dephosphorylation of the GluR1 subunit of AMPA receptors in hippocampus. *Neuron* 21(5):1151–1162.
44. Terashima A, et al. (2008) An essential role for PICK1 in NMDA receptor-dependent bidirectional synaptic plasticity. *Neuron* 57(6):872–882.
45. Yasuda R, et al. (2004) Imaging calcium concentration dynamics in small neuronal compartments. *Sci STKE* 2004(219):pl5.